A&A 608, A81 (2017)
DOI: 10.1051/0004-6361/201730945

Astronomy & Astrophysics

The profile of the bending mode band in solid CO_2

G. A. Baratta and M. E. Palumbo

INAF-Osservatorio Astrofisico di Catania, via Santa Sofia 78, 95123 Catania, Italy
e-mail: mepalumbo@oact.inaf.it

Received 6 April 2017 / Accepted 7 August 2017

ABSTRACT

Context. Solid carbon dioxide (CO_2) is one of the most abundant species detected in icy grain mantles in dense molecular clouds. Its identification is based on the comparison between astronomical and laboratory spectra. In the past 30 yr the profile of solid CO_2 infrared absorption bands has been extensively studied experimentally, however, the debate on the structure (amorphous versus crystalline) of CO_2 samples obtained in laboratory by the thin-film technique is still open.
Aims. The aim of this work is to investigate if the presence of the double peak feature in the profile of the CO_2 bending mode band is related to the crystalline or amorphous structure of the sample.
Methods. We performed new laboratory experiments depositing CO_2 under ultra high vacuum (UHV) conditions at 17 K. We investigated, using infrared transmission spectroscopy, the influence of various experimental parameters on the profile of the CO_2 bands, namely deposition rate, sample thickness, annealing, and presence of H_2O, CH_3OH or CO co-deposited with CO_2.
Results. We found that, within experimental uncertainties, under UHV conditions the profile of the CO_2 bands in pure solid samples does not depend on the deposition rate or the sample thickness in the ranges investigated. In all cases the bending mode band profile shows a double peak (at 660 and 655 cm^{-1}). The spectra also show the Fermi resonance features that cannot be active in crystalline samples. On the other hand, when a small fraction of H_2O or CH_3OH is co-deposited with CO_2 the double peak is not observed while it is observed when a CO_2:CO mixture is considered. Furthermore, we measured the density of solid CO_2 and the refractive index (at 543.5 nm) at 17 K and at 70 K: ρ(17 K) = 1.17 g cm^{-3}, ρ(70K) = 1.49 g cm^{-3}, n(17K) = 1.285, and n(70K) = 1.372.
Conclusions. Our experimental results indicate that the presence of the double peak in the profile of the bending mode band is not an indication of a crystalline structure of the sample and they do not exclude the presence of amorphous solid CO_2 in space.

Key words. astrochemistry – methods: laboratory: solid state – techniques: spectroscopic – ISM: molecules – solid state: volatile – infrared: ISM

1. Introduction

Solid carbon dioxide (CO_2) is one of the most abundant species detected in icy grain mantles in dense molecular clouds. Its abundance with respect to H_2O ranges between 10 and 50% towards different lines of sight (Gerakines et al. 1999; Nummelin et al. 2001; Pontoppidan et al. 2008; Boogert et al. 2015).

In the past 30 yr the profile of solid CO_2 bands has been extensively studied by many groups involved in the experimental investigation of astrophysical ice analogues (e.g. Sandford & Allamandola 1990; Hudgins et al. 1993; Gerakines et al. 1995; Ehrenfreund et al. 1997a,b; Baratta & Palumbo 1998; Palumbo et al. 1998; Dartois et al. 1999; Baratta et al. 2000; Palumbo & Baratta 2000; Ioppolo et al. 2009, 2013; Isokoski et al. 2013; Sivaraman et al. 2013; Escribano et al. 2013; Gerakines & Hudson 2015; Cooke et al. 2016). Previous studies are also available such as Wood & Roux (1982) and Falk (1987).

Sandford & Allamandola (1990) found that the mid-infrared spectrum of a thin CO_2 film at 10 K shows five absorption bands, namely the $^{12}CO_2$ asymmetric stretching mode (ν_3) at about 2343 cm^{-1}, $^{13}CO_2$ asymmetric stretching mode at about 2283 cm^{-1}, $^{12}CO_2$ bending mode (ν_2) with a structured feature peaked at 660 and 655 cm^{-1}, and combination modes $\nu_1+\nu_3$ and $2\nu_2+\nu_3$ at 3707 cm^{-1} and 3600 cm^{-1}, respectively. In their investigation, these authors also showed how the profile of the CO_2 bands depends on the sample composition and temperature. Their samples were obtained in a high vacuum chamber (base pressure of about 3×10^{-8} mbar) and typically deposited on a CsI substrate at a rate of about 2 μm/h. Transmission infrared spectra were taken at normal incidence; that is the IR beam was perpendicular to the surface of the sample.

The ν_1 symmetric stretching vibration, which occurs at about 1385 cm^{-1}, is infrared inactive. However, thick CO_2 samples show two features at about 1385 cm^{-1} and at about 1280 cm^{-1}. These features are assigned to the ν_1 mode in Fermi resonance with the $2\nu_2$ (overtone) mode (Falk 1987; Sivaraman et al. 2013; Gerakines & Hudson 2015).

Baratta & Palumbo (1998) showed that when transmission spectra of pure CO_2 solid samples are taken at oblique incidence the ν_3 band profile shows an additional feature at about 2378 cm^{-1} and the ν_2 band profile shows an additional feature at about 675 cm^{-1}. This occurrence is referred to as the longitudinal optical-transverse optical (LO-TO) splitting. When a polarizer is placed in the path of the IR beam of the spectrometer it is possible to acquire spectra with the electric vector parallel to the plane of incidence (P polarization) and spectra with the electric vector perpendicular to the plane of incidence (S polarization). Baratta & Palumbo (1998) showed that the LO-TO splitting is observed in P polarization spectra while only the TO modes are present in S polarization spectra.

When thin films of pure CO_2 are analysed by reflection absorption infrared spectroscopy, for both ν_3 and ν_2 bands only the

LO mode is detected, while thick films show both the LO and TO modes (e.g. Escribano et al. 2013; Cooke et al. 2016).

Isokoski et al. (2013) performed a detailed study of the CO_2 band profiles recording transmission spectra at resolution 0.1 cm^{-1}. In their experiments the growth rate is determined by setting the exposure to $\sim 10^{16}$ molecules $cm^{-2}\,s^{-1}$. Assuming a density value of 1.17 g cm^{-3} (this work) this corresponds to about 22 μm/h.

Recently, former experimental results have been questioned by Gerakines & Hudson (2015). They have found that the CO_2 bending mode band shows the double peak structure when the sample is obtained with a high deposition rate (>0.2 μm/h), while they do not observe the double peak when the sample is obtained with a low deposition rate (~0.1 μm/h). Based on these experimental results they have claimed that in the former case a crystalline sample is obtained, while in the latter case the sample is amorphous and they have concluded that all previous studies have dealt with crystalline CO_2 samples since a high deposition rate has been adopted.

Other authors have investigated the properties of CO_2 monomers and dimers trapped in various matrices (such as Ar and N_2) at cryogenic temperatures (e.g. Vigasin et al. 2000; Gómez Castaño et al. 2008). In fact weak intermolecular interaction between carbon dioxide molecules results in the formation of van der Waals complexes or dimers. These studies have shown that in a monomer, the ν_2 bending mode is doubly degenerate. In a dimer, this mode splits into four vibrations. Of these, two vibrations, one in-plane and one out-of-plane, are active in infrared absorption (Vigasin et al. 2000). In their work, Gómez Castaño et al. (2008) assigned the band peaked at 1384.1 cm^{-1}, observed when CO_2 is diluted in Ar matrix, to the CO_2 symmetric stretching mode in the dimer. As predicted by theoretical calculations, this mode, which is IR silent in the monomer, is slightly activated in the dimeric structure. The other band at 1278.9 cm^{-1} is attributed to the overtone of the bending mode, which is affected by Fermi resonance. These authors also observed these doublet for the $(CO_2)_2$ isolated in N_2 matrices at 1384.5 and 1279.2 cm^{-1}, respectively.

To further analyse the profile of the band in pure solid CO_2 and the structure of the corresponding CO_2 samples here we performed new experiments depositing CO_2 under ultra high vacuum (UHV) conditions. We investigated, using infrared transmission spectroscopy, the influence of different experimental parameters, namely the deposition rate, sample thickness, annealing, and presence of H_2O, CH_3OH or CO co-deposited with CO_2.

2. Experimental methods

We obtained the experimental results presented here at the Laboratorio di Astrofisica Sperimentale at INAF–Osservatorio Astrofisico di Catania (Italy). The experiments were performed in a stainless steel UHV chamber with a base pressure better than 10^{-9} mbar. A closed-cycle helium cryostat is attached to the UHV chamber for cooling the substrate. The cryostat is protected by a copper shield kept at 77 K. An infrared transparent substrate (KBr) is placed in thermal contact with the final tail of the cryostat and its temperature can be varied between 17 K and 300 K.

The vacuum chamber is placed in the sample compartment of a Fourier transform infrared spectrometer (Bruker Vertex 70) and transmission spectra of the sample are acquired in the range 7800–400 cm^{-1} (1.3–25 μm) at a resolution of 1 cm^{-1} with a sampling of 0.25 cm^{-1}. The substrate forms an angle of 45° with respect to the IR beam. A schematic view of the vacuum chamber is presented in Fig. 1.

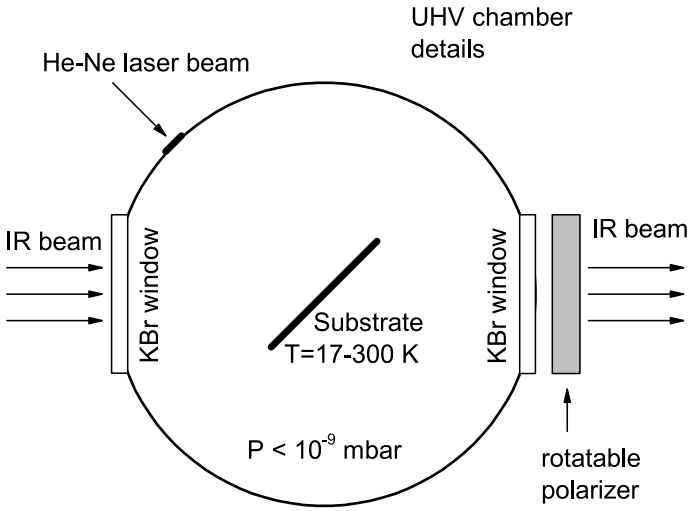

Fig. 1. Schematic depiction of the ultra high vacuum chamber.

Gas or gas mixtures can be admitted into the main chamber by means of a needle valve. Because of the cold surface of the substrate, gas (or mixtures) are subsequently deposited as solids. The gas inlet is not directed towards the substrate, thus a background deposition is obtained. This method has the advantage that the film deposited has a uniform thickness but has the disadvantage that gas phase molecules can freeze out onto all cold surfaces inside the chamber. To avoid any deposition on the backside of the substrate, this is protected by a 2 cm long copper tube aligned with the IR beam and with the central hole with a diameter of about 4 mm.

A He-Ne laser (λ = 543.5 nm) is used to monitor the sample thickness on the substrate during accretion. This is achieved by looking at the interference pattern (intensity versus time) given by the laser beam reflected at near normal incidence (2.9°) by the vacuum-film and film-substrate interfaces. More details on this procedure can be found in Baratta & Palumbo (1998), Fulvio et al. (2009), Modica & Palumbo (2010), and Urso et al. (2016).

A rotatable polarizer is placed in the path of the IR beam, which enables us to subsequently record spectra in P mode, in which the electric vector is parallel to the plane of incidence, and S mode, in which the electric vector is perpendicular to the plane of incidence. The plane of incidence is the plane of the paper in Fig. 1. Background spectra are recorded at the start of the measurement before sample deposition in both modes and subsequently each spectrum is divided by the background spectrum acquired in the same polarization mode.

A list of the new experiments performed in this work is given in Table 1. Aldrich Chemical 99.8% CO_2, 99.0% CO, Sigma Aldrich Chromasolv Plus H_2O, and Merck 99.8% CH_3OH were used to prepare the samples. The CO_2:X ratio in samples numbered from 6 to 9 in Table 1 is determined on the basis of previous calibration experiments and this ratio resulted to be consistent with the column density ratio estimated from the spectra adopting A(CO_2, 2340) = 7.6×10^{-17} cm mol^{-1} (Yamada & Person 1964), A(CO_2, 660) = 1.1×10^{-17} cm mol^{-1} (Gerakines et al. 1995), A(H_2O, 1660) = 1×10^{-17} cm mol^{-1} (Hudgins et al. 1993), A(CO) = 1.1×10^{-17} cm mol^{-1} (Jiang et al. 1975), and A(CH_3OH, 1020) = 1.3×10^{-17} cm mol^{-1} (Palumbo et al. 1999). Figure 2 shows the

Table 1. New experiments performed in this work.

Sample no.	Composition	Deposition rate (μm/h)	Thickness (μm)	Bending mode double peak
1	pure CO_2	0.110	0.150	yes
2	pure CO_2	0.065	0.125	yes
3	pure CO_2	0.100	0.652	yes
4	pure CO_2	0.100	0.143	yes
5	pure CO_2	0.076	0.108	yes
6	CO_2:H_2O = 12:1	0.067	0.122	no
7	CO_2:H_2O = 12:1	0.950	0.123	no
8	CO_2:CO = 8:1	0.107	0.155	yes
9	CO_2:CH_3OH = 11:1	0.112	0.149	no

Notes. All samples were deposited at 17 K other than sample No. 5, which was deposited at 70 K.

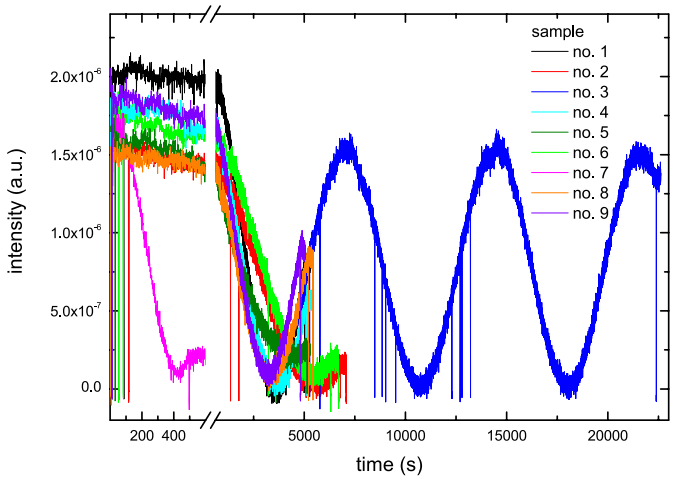

Fig. 2. Interference curves acquired during deposition of all the samples studied in this work.

interference curves acquired during deposition of all the samples studied in this work.

3. Results

3.1. Refractive index and density measurement

From the interference curve obtained during deposition of sample No. 3 (final thickness equal to 0.652 μm) it has been possible to calculate the refractive index of solid CO_2 (at 543.5 nm) and its density at 17 K. In fact the amplitude of the experimental interference curve depends on the refractive index n_f of the species at laser wavelength, the refractive index n_s of the substrate, the incidence angle θ_i of the laser beam, and the polarization of the laser light. Hence, because all the other quantities are known, n_f can be derived, using numerical methods, from the measured amplitude of the experimental interference curve (intensity ratio between maxima and minima). This was achieved via a program, written in Fortran language (Baratta & Palumbo 1998)[1]. The value we obtained is n_{CO_2} = 1.285 at 543.5 nm.

[1] A free web interface that allows the online use of the program is available at http://www.oact.inaf.it/thickness/ (Urso et al. 2016).

From the derived n_f value, we estimated the film density using the Lorentz-Lorenz relation. In particular, for a given species the Lorentz-Lorenz coefficient, L, is nearly constant for a fixed wavelength regardless of the material phase and temperature (Wood & Roux 1982). This quantity is related to the density (ρ) by the Lorentz-Lorenz relation

$$L\rho = \frac{n_f^2 - 1}{n_f^2 + 2}. \quad (1)$$

Adopting L = 0.153 cm^3/g, we obtained $\rho(CO_2)$ = 1.17 g cm^{-3} at 17 K. The value L = 0.153 cm^3/g was obtained from the refractive index at 543.5 nm (n = 1.0004504) measured at standard conditions (0 °C and 760 Torr) as reported by Polyanskiy (2017). Recently, Loeffler et al. (2016) have presented a detailed study on the effects of the deposition technique on the measurements of the visible (λ = 670 nm) refractive index and the density of solid CO_2. Fitting their experimental data they have found that the Lorentz-Lorenz coefficient values L = 0.148 ± 0.006 cm^3/g. Neglecting the small differences in the value of L due to the different wavelength, the value obtained by Loeffler et al. (2016) is, within uncertainties, equal to the value obtained from gas phase measurements, confirming that the Lorentz-Lorenz coefficient is nearly constant regardless of the material phase and temperature.

Following the same procedure, from the interference curve obtained during deposition of sample No. 5, we estimated the refractive index of solid CO_2 (at 543.5 nm) and its density at 70 K. We found n_{CO_2} = 1.372 and $\rho(CO_2)$ = 1.49 g cm^{-3}.

We point out that different values of the density and refractive index for solid CO_2 have been reported in the literature. Satorre et al. (2008) measured the density and refractive index (at 632.8 nm) of CO_2 at various temperatures (from 10 K to its sublimation temperature) and found that the density varies from 0.98 g cm^{-3} (at 10 K) to 1.5 g cm^{-3}, while the refractive index varies from 1.21 to 1.35. Wood & Roux (1982) measured a density value of 1.08 g cm^{-3} and refractive index (at 632.8 nm) equal to 1.27 at 20 K. Loeffler et al. (2016) have found that at 14 K the refractive index varies in the range 1.27–1.31 and the density varies in the range 1.18–1.38 g cm^{-3} depending on the deposition technique. As pointed out by Loeffler et al. (2016), it is not surprising that different measurements result in different values. In fact the density and in turn the refractive index of a solid sample in some instances strongly depend on the experimental conditions such as temperature, growth angle, and deposition rate

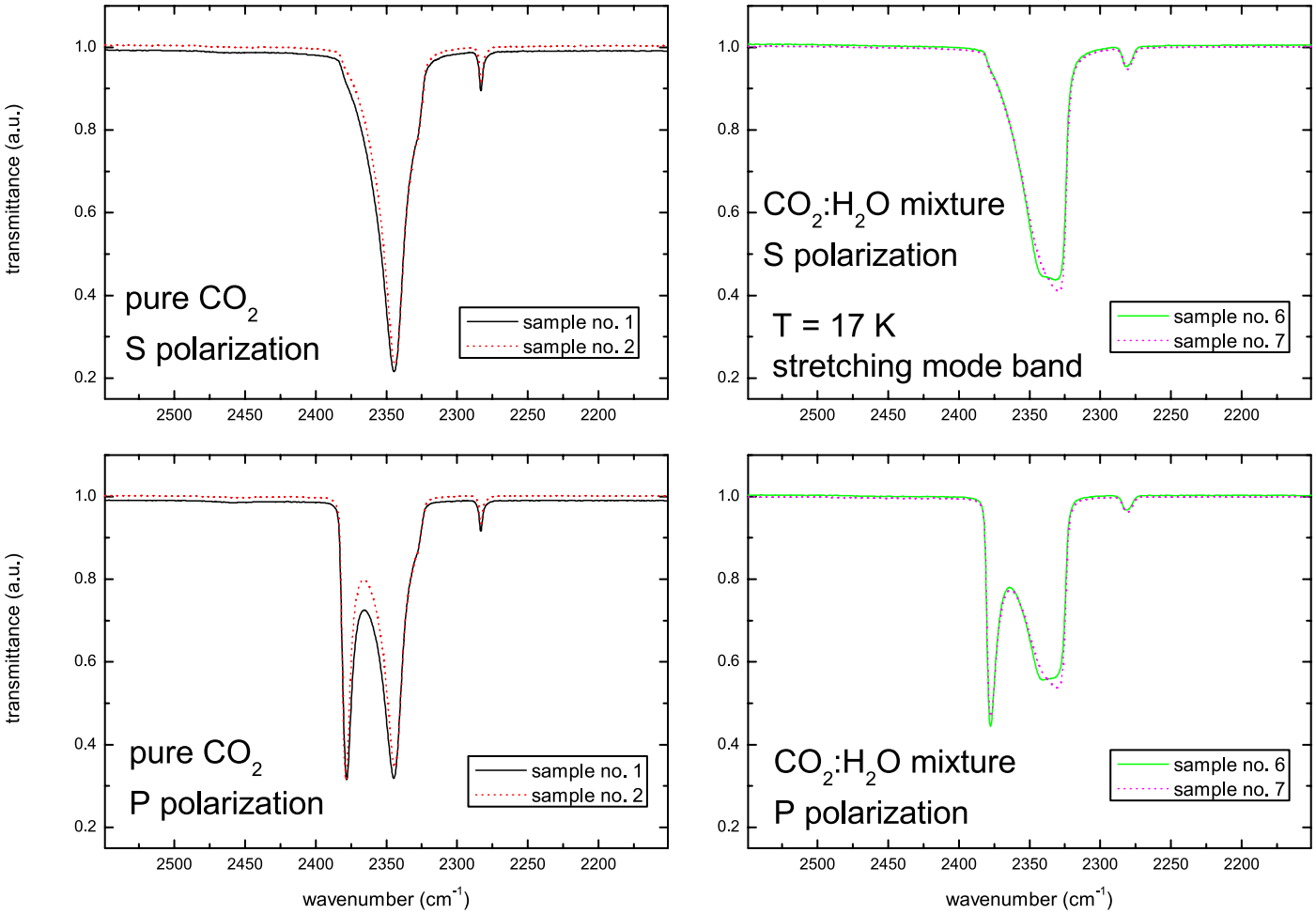

Fig. 3. Stretching mode band of CO_2 in pure solid CO_2 and CO_2:H_2O mixtures. Spectra are taken at 17 K and are shown in transmittance scale.

(e.g. Hagen et al. 1983; Jenniskens & Blake 1994; Kimmel et al. 2001a,b; Dohnálek et al. 2003).

3.2. Pure CO_2 and CO_2:H_2O mixtures

Figure 3 shows the profile of the stretching mode band of samples 1, 2 (pure solid CO_2), 6, and 7 (CO_2:H_2O mixtures) in P and S polarization. For samples Nos. 1 and 2 (pure solid CO_2), spectra taken in S polarization (top panel) show a band centred at about 2345 cm^{-1} that is assigned to the asymmetric stretching mode (ν_3) of $^{12}CO_2$ and a band centred at about 2283 cm^{-1} that is assigned to the asymmetric stretching mode of $^{13}CO_2$. Spectra taken in P polarization (bottom panel) show an additional band centred at about 2378 cm^{-1} that is assigned to the LO mode of the $^{12}CO_2$ asymmetric stretching mode. As discussed by Baratta & Palumbo (1998), Palumbo & Baratta (2000), Palumbo et al. (2006), and Urso et al. (2016) when transmission spectra are taken at oblique incidence, spectra in P polarization show the LO-TO splitting while spectra taken in S polarization, for symmetry reasons, are equivalent to spectra taken at normal incidence and only show the TO mode. When a small amount of H_2O is present in the mixture (i.e. samples Nos. 6 and 7) the peak position of the ν_3 band shifts to 2330 cm^{-1} and the band is broader (panels on the right-hand side of Fig. 3).

Figure 4 shows the profile of the bending mode band of samples 1, 2, 3 (pure solid CO_2), 6, and 7 (CO_2:H_2O mixtures) in P and S polarization. For samples Nos. 1, 2, and 3 (i.e. pure solid CO_2) spectra taken in S polarization (top panel) show a double peak band centred at 660 and 655 cm^{-1} that is assigned to the bending mode (ν_2) of $^{12}CO_2$ and a band centred at about 639 cm^{-1} that is assigned to the bending mode of $^{13}CO_2$. Spectra taken in P polarization (bottom panel) show an additional band centred at about 675 cm^{-1} that is assigned to the LO mode of the $^{12}CO_2$ bending mode. For samples Nos. 6 and 7 (i.e. CO_2:H_2O mixtures) spectra taken in S polarization (top panel) show a single peak band centred at 655 cm^{-1} that is assigned to the bending mode (ν_2) of $^{12}CO_2$. Spectra taken in P polarization (bottom panel) show an additional band centred at about 675 cm^{-1} that is assigned to the LO mode of the $^{12}CO_2$ bending mode.

Figure 5 shows the spectral range 4000–2800 cm^{-1} for samples No. 2 (pure solid CO_2) and No. 6 (CO_2:H_2O mixture). These samples have the same thickness ($\simeq$0.12 μm). The spectrum of sample No. 2 shows two features at 3708 and 3600 cm^{-1} easily assigned to the $\nu_1+\nu_3$ and $2\nu_2+\nu_3$ combination modes (e.g. Sandford & Allamandola 1990) of solid CO_2. The spectrum of sample No. 6 shows two features at 3704 and 3597 cm^{-1} that are less intense and broader with respect to the corresponding features in sample No. 2. These differences can be ascribed to the presence of H_2O in sample No. 6. It is important to note that none of the spectra show the feature due to polymeric water at about 3300 cm^{-1}.

Figure 6 shows the spectral range 1530–1180 cm^{-1} for sample No. 3 (thick pure solid CO_2). This spectrum clearly shows two features at 1384 cm^{-1} and at about 1278 cm^{-1}. These features are assigned to the ν_1 (symmetric stretching

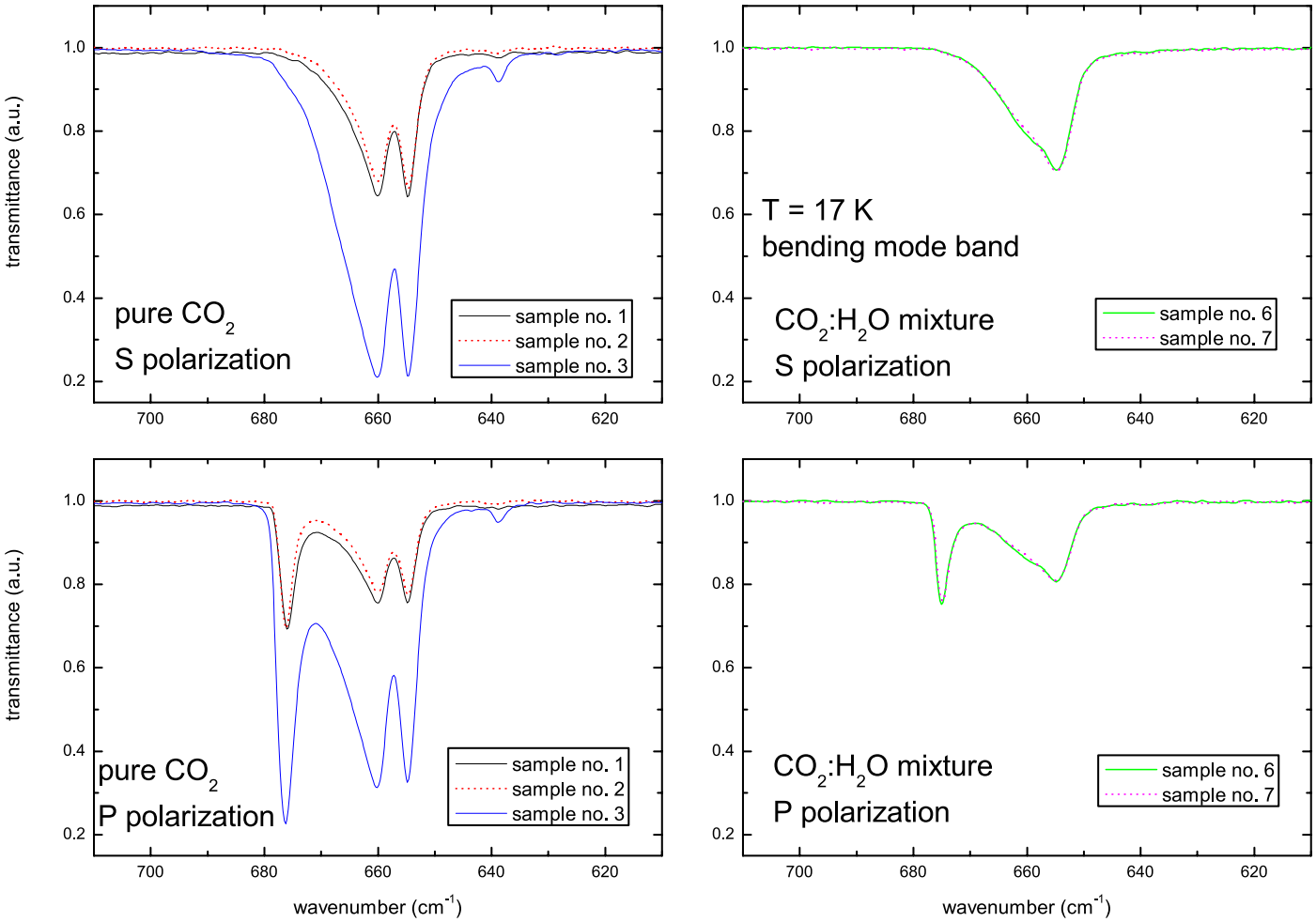

Fig. 4. Bending mode band of CO_2 in pure solid CO_2 and CO_2:H_2O mixtures. Spectra, acquired at 17 K, are shown in transmittance scale.

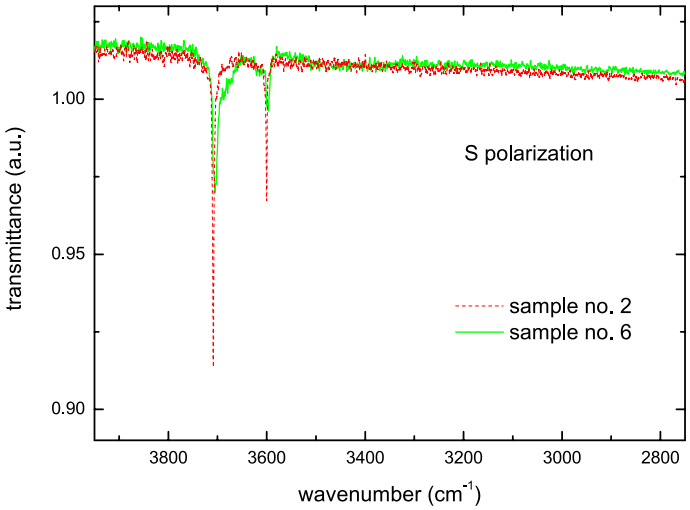

Fig. 5. Transmittance spectra of samples Nos. 2 and 6 in the 4000–2800 cm^{-1} spectral region. Spectra are acquired at 17 K.

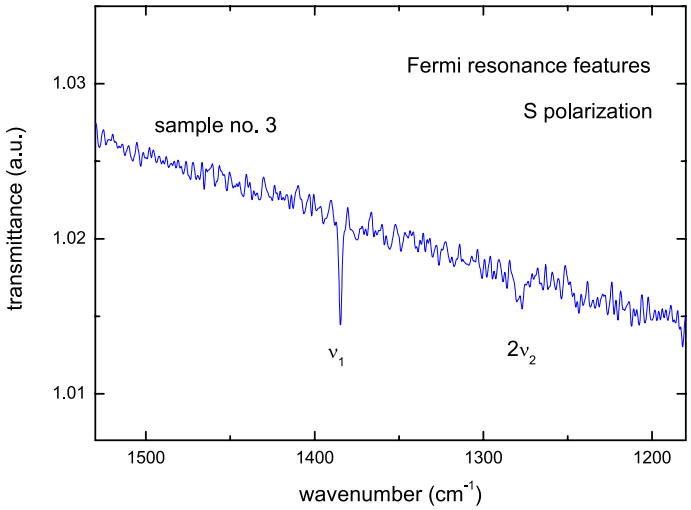

Fig. 6. Fermi resonance features for sample No. 3 (thick pure CO_2). The spectrum is acquired at 17 K and is shown in transmittance scale.

vibration) mode in Fermi resonance with the $2\nu_2$ (overtone) mode (Falk 1987). According to previous studies, these features are observed in amorphous samples while they are not detected in crystalline samples (Falk 1987; Sivaraman et al. 2013; Gerakines & Hudson 2015).

3.3. CO_2:CO and CO_2:CH_3OH mixtures

In order to further investigate the behaviour of CO_2 when a small fraction of H_2O (μ = 1.85 debye) is present in the sample, we analysed mixtures with CO (μ = 0.12 debye) and CH_3OH (μ = 1.69 debye). Figure 7 shows the profile of the asymmetric

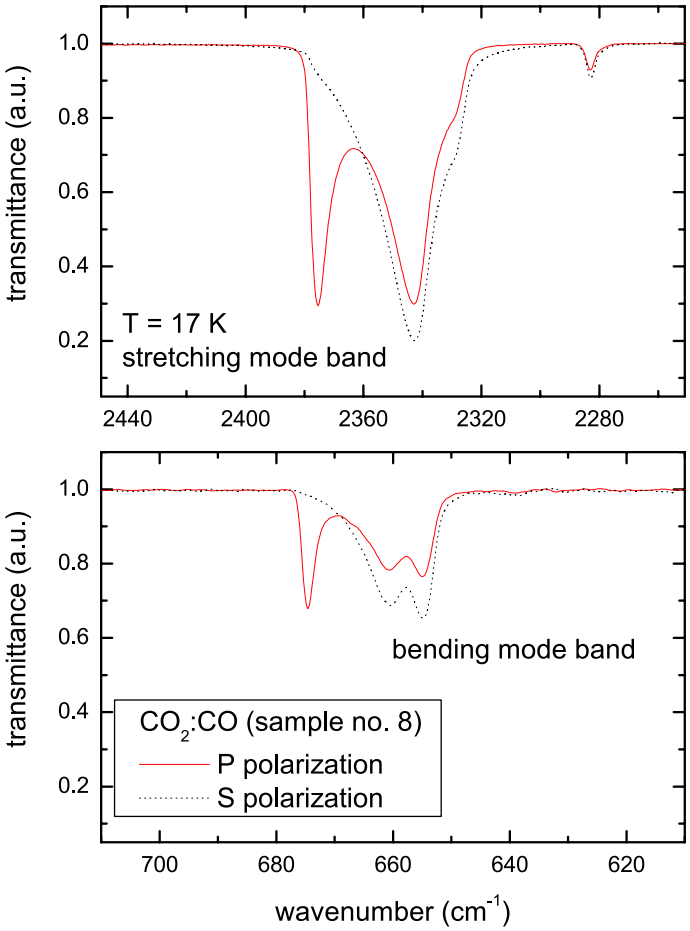

Fig. 7. Transmittance spectra of sample No. 8 (CO_2:CO = 8:1 mixture) in the 2450–2250 cm^{-1} spectral region (*top panel*) and in the 710–610 cm^{-1} spectral region (*bottom panel*). Spectra are acquired at 17 K.

stretching mode and the bending mode bands in a CO_2:CO = 8:1 mixture at 17 K. The asymmetric stretching mode band peaks at 2343 cm^{-1} (TO mode) and the LO mode observed in P-polarization spectra peaks at 2375 cm^{-1}. The profile of the bending mode band shows a double peak (660 and 655 cm^{-1}) and in P-polarization spectra the LO mode peaks at 675 cm^{-1}. In this mixture the profile of the CO_2 bands is very similar to the profile of the same bands in pure CO_2 sample (see Figs. 3 and 4).

Figure 8 shows the profile of the asymmetric stretching mode and the bending mode bands in a CO_2:CH_3OH = 11:1 mixture. In the spectrum taken after sample deposition at 17 K (S polarization) the asymmetric stretching mode band peaks at 2330 cm^{-1} and the LO mode observed in the spectrum taken in P polarization peaks at 2376 cm^{-1}; the bending mode band does not show (at 17 K) the double peak structure and peaks at 655 cm^{-1} and the LO mode peaks at 674 cm^{-1}. In this case the profile of the CO_2 bands is very similar to the profile of the same bands in a CO_2:H_2O = 12:1 mixture (see Figs. 3 and 4).

3.4. Thermal annealing

Figure 9 presents the profile of CO_2 asymmetric stretching and bending mode bands for a sample of pure CO_2 (sample No. 4) deposited at 17 K, warmed up to 77 K, and cooled down the 17 K. Similar to the results presented by other authors (e.g. Sandford & Allamandola 1990; Isokoski et al. 2013), the figure shows that both band profiles become narrower and deeper upon thermal annealing while no changes are observed when the sample is cooled down to 17 K. In fact the spectra (both P and S polarization) taken after the sample is cooled down to 17 K are indistinguishable from the respective spectra taken at 77 K.

Figure 10 presents the profile of CO_2 asymmetric stretching and bending mode bands for a sample of pure CO_2 (sample No. 5) deposited at 70 K, warmed up to 77 K, and cooled down to 17 K. The spectra shown (both P and S polarization) are indistinguishable from each other.

These results indicate that the structure of the CO_2 sample deposited at 17 K is amorphous (unstable) and evolves, upon annealing, to a stable crystalline structure that is not further modified when the sample is cooled down. On the other hand, the sample deposited at 70 K does not show any variation upon thermal cycles suggesting that the sample deposited at 70 K has a stable crystalline structure. A similar behaviour has been observed for other solid phase molecules (e.g. Hudgins et al. 1993; Leto & Baratta 2003). The difference between the structure of the sample deposited at 17 K and that of the sample deposited at 70 K is also testified by the different values of the refractive index and density measured (see Sect. 3.1).

Figure 8 shows the profile of the CO_2 bands when a CO_2:CH_3OH mixture (sample No. 9) deposited at 17 K is warmed up to 77 K and then cooled down to 17 K. In this case, upon thermal annealing, the profile of the CO_2 bands significantly changes. At 77 K the stretching mode band and the bending mode band profiles both shift to higher wave numbers and become narrower. Furthermore, the profile of the bending mode band splits into two components. When the sample is cooled down to 17 K it is not further modified and the spectra taken at 17 K (both P and S polarization) are indistinguishable from the respective spectra taken at 77 K.

4. Discussion

The experimental results presented here indicate that when pure CO_2 is deposited on a cold substrate at low temperature in a UHV chamber the IR spectrum simultaneously shows the Fermi resonance features and the double peak of the bending mode band profile. As discussed by Falk (1987), Sivaraman et al. (2013), and Gerakines & Hudson (2015), the Fermi resonance features are observed in amorphous samples while they are not detected in crystalline samples. As a consequence the IR spectrum of amorphous pure solid CO_2 shows the double peak of the bending mode band profile. The double peak profile disappears when or a small amount of CH_3OH or a small amount of H_2O (as small as 10%), which is not detectable by the band at 3300 cm^{-1} assigned to polymeric water, is co-deposited with CO_2 (as shown in Figs. 4 and 8). H_2O and CH_3OH are polar molecules (dipole moment equal to 1.85 and 1.69 debye, respectively); our results show that when a small amount of an apolar molecule (such as CO, μ = 0.12 debye) is co-deposited with CO_2 the profile of the CO_2 bands does not change significantly.

Öberg et al. (2007) have studied the effects of CO_2 on H_2O band profiles and band strength values in solid H_2O:CO_2 mixtures and have found that the band strength of the OH stretching mode (at about 3300 cm^{-1}) decreases as much as an order of magnitude from a sample of pure H_2O to a H_2O:CO_2 = 1:4 solid sample. They have not reported the results for mixtures with a lesser abundance of H_2O mixed with CO_2 but, from the decreasing trend reported, it is reasonable to assume that the band strength of the OH stretching mode band would further decrease

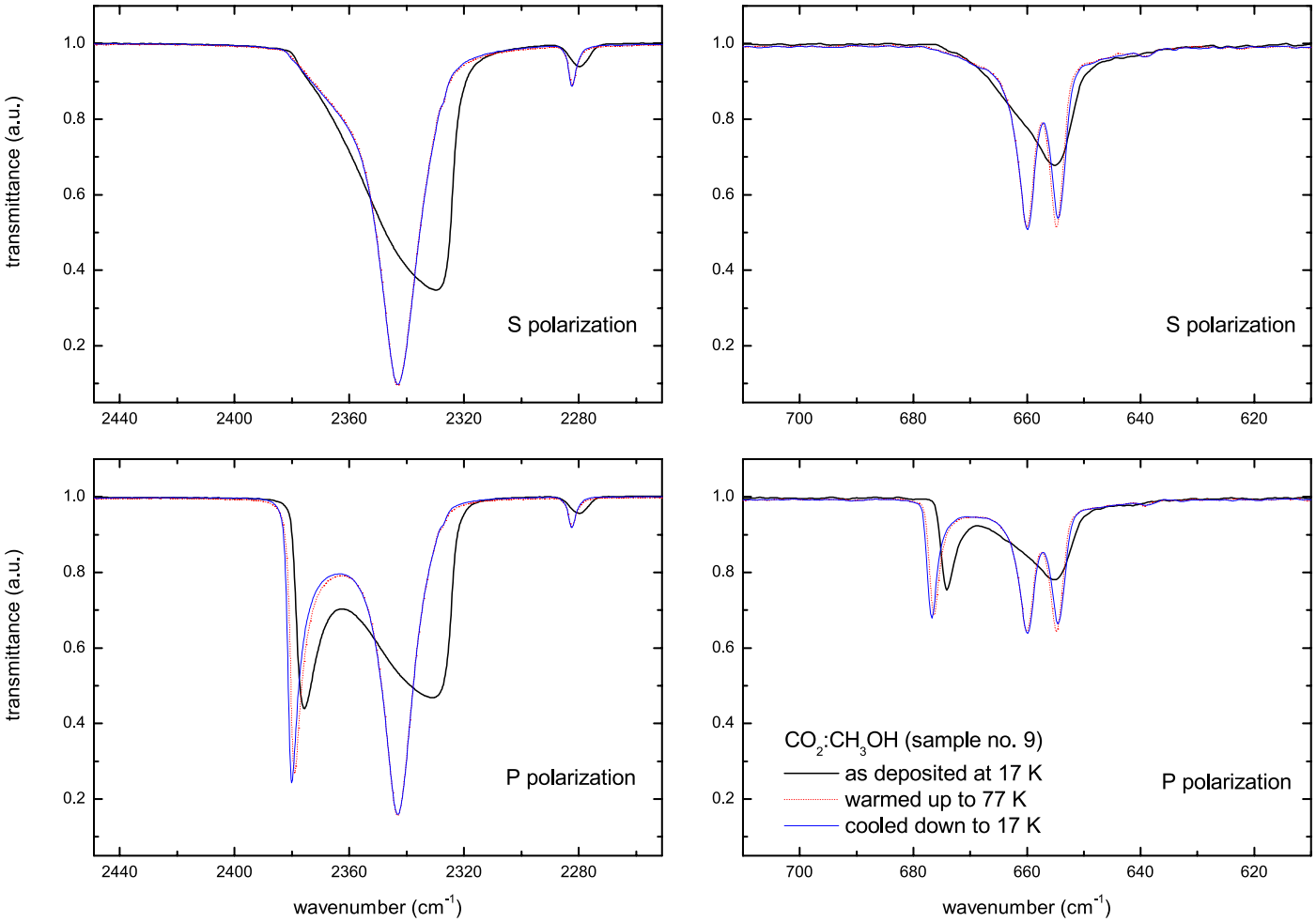

Fig. 8. Transmittance spectra of sample No. 9 (CO_2:CH_3OH = 11:1 mixture) in the 2450–2250 cm^{-1} spectral region (*left-hand panels*) and in the 710–610 cm^{-1} spectral region (*right-hand panels*). Spectra are acquired after sample deposition at 17 K, after thermal annealing to 77 K and after cooling down to 17 K.

in more diluted mixtures (such as the H_2O:CO_2 ~ 1:10 mixture considered here). As shown in Fig. 5 the spectrum of a CO_2:H_2O = 12:1 mixture does not show the band due to polymeric water at 3300 cm^{-1}. This evidence is consistent with the results reported by Öberg et al. (2007).

Gerakines & Hudson (2015) have performed their experiments in a high vacuum chamber (base pressure 10^{-7}–10^{-8} Torr). As reported in their manuscript, "the chief contaminant seen was residual H_2O from the CO_2 reagents and possibly from the vacuum system. Trace amounts of H_2O gave weak IR peaks (<0.01 absorbance units in all cases) in the 3700–3500 and 1600 cm^{-1} regions". The deposition rate used was 0.1 μm/h. The substrate temperature was 10 K. In those experimental conditions they have not observed the double peak of the bending mode profile in the spectrum of pure solid CO_2. When the deposition rate was doubled (i.e. about 0.2 μm/h) the double peak has been observed. Gerakines & Hudson (2015) have interpreted these experimental results as due to amorphous (slow deposition rate) and crystalline (fast deposition rate) samples. On the basis of the experimental results reported in the present manuscript, the results of Gerakines & Hudson (2015) could be interpreted as due to a higher presence of water contamination in the sample obtained with a slow deposition rate. In fact when the deposition rate is slowed down the relative contribution of the background residual gas (mainly H_2O) increases.

Here we presented the spectrum of a sample obtained with a deposition rate of 0.065 μm/h (sample No. 2), that is about half the slow deposition rate adopted by Gerakines & Hudson (2015). As shown in Fig. 4 the profile of the CO_2 bending mode shows the double peak. An even lower deposition rate (about 0.03 μm/h) was adopted by Escribano et al. (2013) who have observed the double peak of the bending mode band[2]. We also present the spectra of two CO_2:H_2O = 12:1 mixtures obtained with a deposition rate of 0.067 μm/h (sample No. 6) and 0.950 μm/h (sample No. 7), respectively. Both spectra (Fig. 4) do not show the double peak of the bending mode. Hence the disappearance of the double peak observed in the bending mode can be ascribed to the presence of H_2O contamination independently of the deposition rate.

Figures 8–10 show the modifications observed in the profile of the asymmetric stretching mode and bending mode bands after warm up. The comparison between the results reported in Figs. 9 and 10 indicates that the structure of the CO_2 sample deposited at 17 K is different from the structure of the sample deposited at 70 K. Furthermore, the results reported in Fig. 8 are very similar to the results reported by Gerakines & Hudson (2015) in their Fig. 2. In their work Gerakines & Hudson (2015)

[2] The deposition rate in units of μm/h has been obtained from the deposition rate of 0.014 ML/s reported by the authors, assuming a density of 1.17 g cm^{-3} (this work).

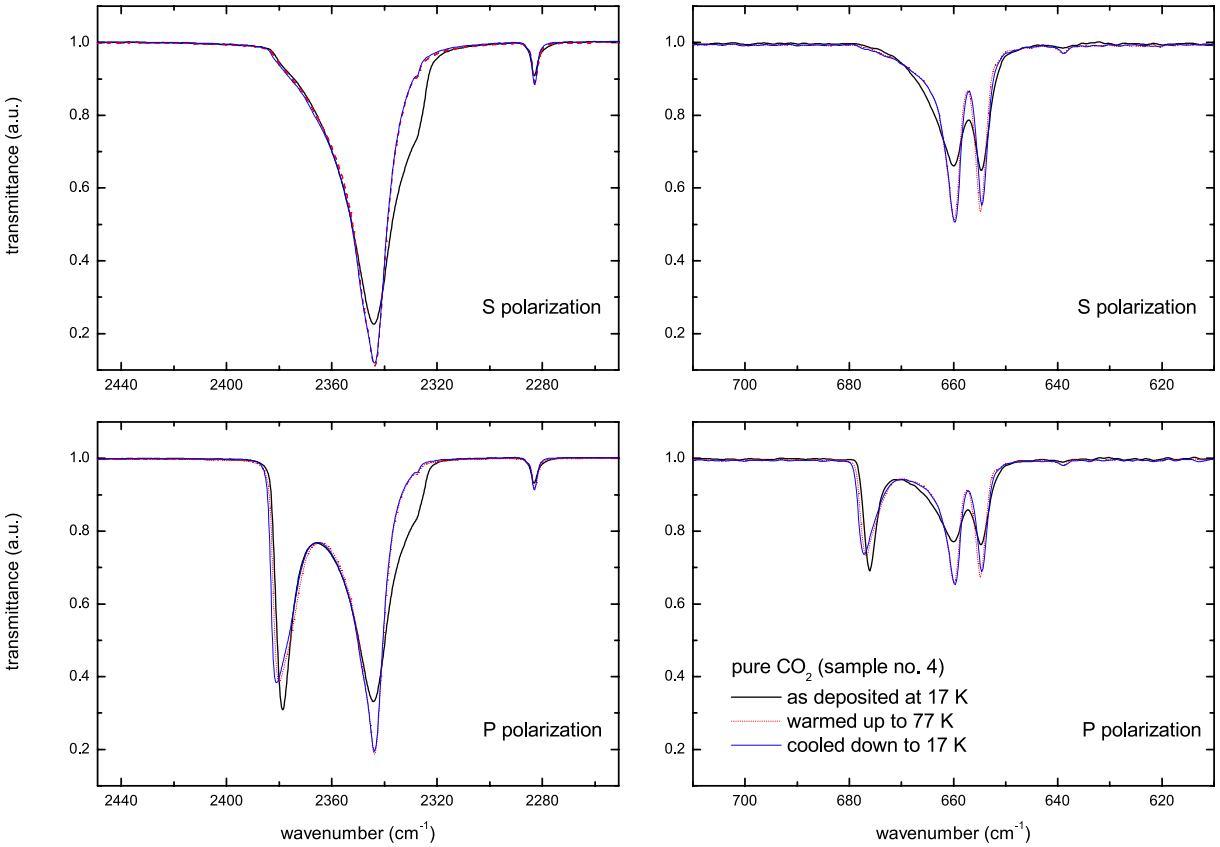

Fig. 9. Transmittance spectra of pure CO_2 (sample No. 4) in the 2450–2250 cm^{-1} spectral region (*left-hand panels*) and in the 710–610 cm^{-1} spectral region *(right-hand panels*). Spectra are acquired after sample deposition at 17 K, after thermal annealing to 77 K and after cooling down to 17 K.

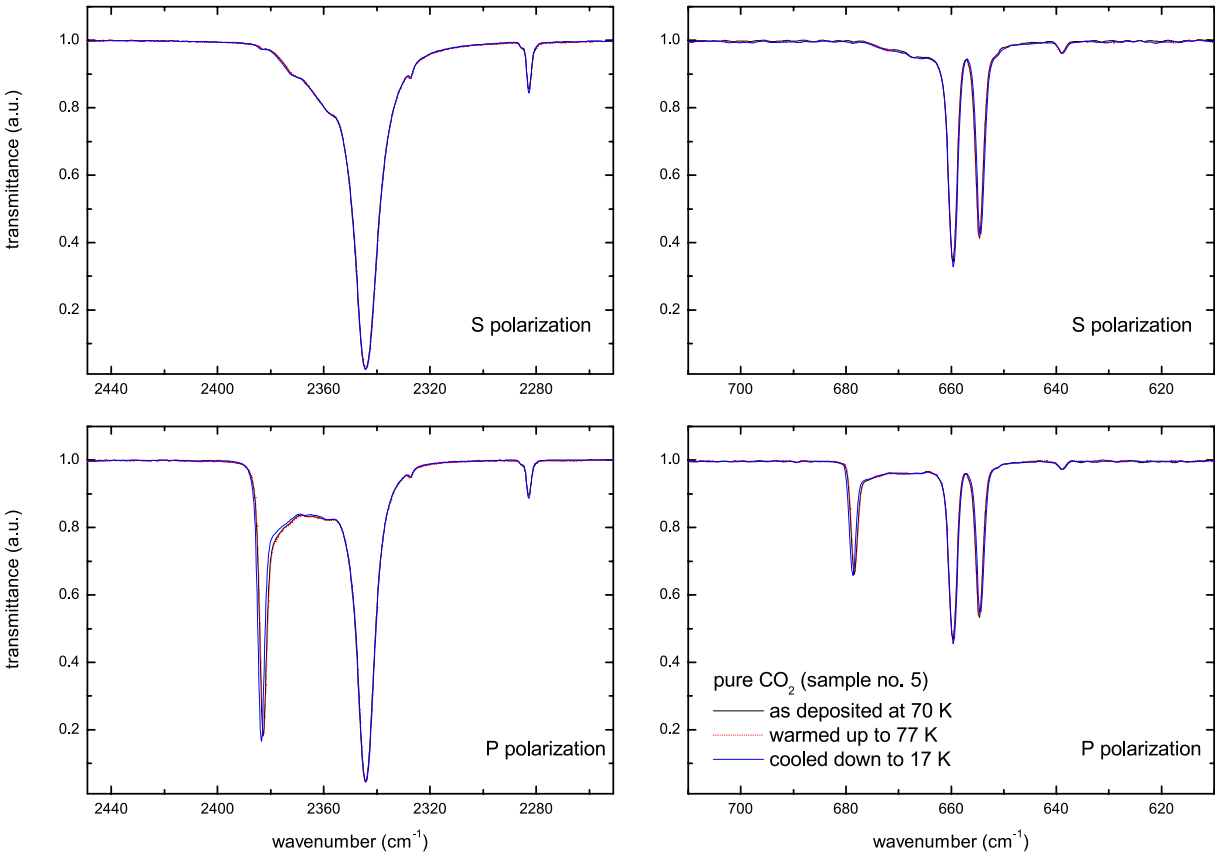

Fig. 10. Transmittance spectra of pure CO_2 (sample No. 5) in the 2450–2250 cm^{-1} spectral region (*left-hand panels*) and in the 710–610 cm^{-1} spectral region (*right-hand panels*). Spectra are acquired after sample deposition at 70 K, after thermal annealing to 77 K and after cooling down to 17 K.

have assumed that they deposited an amorphous CO_2 sample that crystallizes after warm up. On the basis of the results reported in the present manuscript the comparison between the two figures indicates that whichever polar species is co-deposited with CO_2 (either H_2O or CH_3OH) the behaviour of the bands profile after warm up is the same.

A theoretical interpretation of the experimental results presented in this manuscript is beyond the aim of this work. The double peak observed in the profile of the bending mode band in crystalline CO_2 samples is generally ascribed to the Davydov splitting (e.g. Pontoppidan et al. 2008; Isokoski et al. 2013; Cooke et al. 2016). The Davydov splitting (factor-group splitting) is the splitting of bands in the electronic or vibrational spectra of crystals due to the presence of more than one (interacting) equivalent molecular entity in the unit cell. This splitting is then not expected in amorphous disordered samples. Several studies in the field of organic semiconductors have demonstrated that amorphous solids show site splitting analogous to crystal Davydov splitting and that homo-dimers show the Davydov splitting (e.g. Jankowlak et al. 1983; Ottiger et al. 2015). Other studies in the field of atmospheric physics have shown that in a CO_2 monomer, the ν_2 bending mode is doubly degenerate while in a dimer, this mode splits into four vibrations. Of these, two vibrations, one in-plane and one out-of-plane, are active in infrared absorption (Vigasin et al. 2000). Following these results we suggest that during vapor deposition of pure CO_2 samples the formation of dimers takes place, while when a small amount of a polar species (such as H_2O and CH_3OH) is co-deposited with CO_2 the formation of dimers is inhibited. Furthermore, the annealing experiments suggest that the dimers formed during deposition at low temperature are randomly oriented while a more ordered structure is obtained after warm up. This hypothesis is also consistent with the detection of the Fermi resonance features in dimers (e.g. Gómez Castaño et al. 2008) but not in crystalline samples (Falk 1987; Sivaraman et al. 2013; Gerakines & Hudson 2015).

In summary we have found that, within experimental uncertainties, in UHV conditions, the profile of the CO_2 bands in pure solid samples does not depend on the deposition rate or the sample thickness in the ranges investigated. In all cases the bending mode band profile shows a double peak (at 660 and 655 cm^{-1}). The spectra of these samples show the Fermi resonance features that cannot be active in crystalline samples. On the other hand when a small fraction of a polar species (such as H_2O and CH_3OH) is co-deposited with CO_2 the double peak is not observed. Our experimental results indicate that the presence of the double peak in the profile of the CO_2 bending mode is not an indication of a crystalline structure of the solid sample and these results do not exclude that amorphous solid CO_2 is present in space.

Acknowledgements. The authors are grateful to Sergio Ioppolo for stimulating discussions on this work. This research has been partially supported by the Italian Ministero dell'Istruzione, dell'Università e della Ricerca through the grant Progetti Premiali 2012-iALMA (CUP C52I13000140001).

References

Baratta, G. A., & Palumbo, M. E. 1998, J. Opt. Soc. Am. A, 15, 3076
Baratta, G. A., Palumbo, M. E., & Strazzulla, G. 2000, A&A, 357, 1045
Boogert, A. C. A., Gerakines, P. A., & Whittet, D. C. B. 2015, ARA&A, 53, 541
Cooke, I. R., Fayolle, E. C., & Öberg, K. I. 2016, ApJ, 832, 5
Dartois, E., Demyk, K., d'Hendecourt, L. B., & Ehrenfreund, P. 1999, A&A, 351, 1066
Dohnálek, Z., Kimmel, G. A., Ayotte, P., Smith, R. S., & Kay, B. D. 2003, J. Chem. Phys., 118, 364
Ehrenfreund, P., Boogert, A. C. A., Gerakines, P. A., Tielens, A. G. G. M., & van Dishoeck, E. F. 1997a, A&A, 328, 649
Ehrenfreund, P., d'Hendecourt, L., Dartois, E., et al. 1997b, Icarus, 130, 1
Escribano, R. M., Muñoz Caro, G. M., Cruz-Diaz, G. A., Rodríguez-Lazcano, Y., & Maté, B. 2013, PNAS, 110, 12899
Falk, M. 1987, J. Chem. Phys., 86, 560
Fulvio, D., Sivaraman, B., Baratta, G. A., Palumbo, M. E., & Mason, N. J. 2009, Spectrochimica Acta Part A, 72, 1007
Gerakines, P. A., & Hudson, R. L. 2015, ApJ, 808, L40
Gerakines, P. A., Schutte, W. A., Greenberg, J. M., & van Dishoeck, E. F. 1995, A&A, 296, 810
Gerakines, P. A., Whittet, D. C. B., Ehrenfreund, P., et al. 1999, ApJ, 522, 357
Gómez Castaño, J. A., Fantoni, A., & Romano, R. M. 2008, J. Mol. Struct., 881, 68
Hagen, W., Tielens, A. G. G. M., & Greenberg, J. M. 1983, A&AS, 51, 389
Hudgins, D. M., Sandford, S. A., Allamandola, L. J., & Tielens, A. G. G. M. 1993, ApJS, 86, 713
Ioppolo, S., Palumbo, M. E., Baratta G. A., & Mennella, V. 2009, A&A, 493, 1017
Ioppolo, S., Sangiorgio, I., Baratta G. A., & Palumbo, M. E. 2013, A&A, 554, A34
Isokoski, K., Poteet, C. A., & Linnartz, H. 2013, A&A, 555, A85
Jankowlak, R., Rockwitz, K. D., & Bässler, H. 1983, J. Phys. Chem., 87, 552
Jenniskens, P., & Blake, D. 1994, Science, 265, 753
Jiang, G. J., Person, W. B., & Brown, K. G. 1975, J. Chem. Phys., 62, 1201
Kimmel, G. A., Stevenson, K. P., Dohnálek, Z., Smith, R. S., & Kay, B. D. 2001a, J. Chem. Phys., 114, 5284
Kimmel, G. A., Dohnálek, Z., Stevenson, K. P., Smith, R. S., & Kay, B. D. 2001b, J. Chem. Phys., 114, 5295
Leto, G., & Baratta, G. A., 2003, A&A, 397, 7
Loeffler, M. J., Moore, M. H., & Gerakines, P. A. 2016, ApJ, 827, 98
Modica, P., & Palumbo, M. E. 2010, A&A, 519, A22
Nummelin, A., Whittet, D. C. B., Gibb, E. L., Gerakines, P. A., & Chiar, J. E. 2001, ApJ, 558, 185
Öberg, K., Fraser, H. J., Boogert, A. C. A., et al. 2007, A&A, 462, 1187
Ottiger, P., Köpper, H., & Leutwyler, S. 2015, Chem. Sci., 6, 6059
Palumbo, M. E., & Baratta, G. A. 2000, A&A, 361, 298
Palumbo, M. E., Baratta, G. A., Brucato, J. R., et al. 1998, A&A, 334, 247
Palumbo, M. E., Castorina, A. C., & Strazzulla, G. 1999, A&A, 342, 551
Palumbo, M. E., Baratta, G. A., Collings, M. P., & McCoustra, M. R. S. 2006, Phys. Chem. Chem. Phys., 8, 279
Polyanskiy, M. N. 2017, Refractive index database, `https://refractiveindex.info`, accessed on 2017-03-27
Pontoppidan, K. M., Boogert, A. C. A., Fraser, H. J., et al. 2008, ApJ, 678, 1005
Sandford, S. A., & Allamandola, L. J. 1990, ApJ, 355, 357
Satorre, M. A., Domingo, M., Millán, C., et al. 2008, Planet. Space Sci., 56, 1748
Sivaraman, B., Raja Sekhar, B. N., Fulvio, D., et al. 2013, J. Chem. Phys., 139, 074706
Urso, R. G., Sciré, C., Baratta, G. A., Compagnini, G., & Palumbo, M. E. 2016, A&A, 594, A80
Vigasin, A. A., Schriver-Mazzuoli, L., & Schriver, A. 2000, J. Phys. Chem. A, 104, 5451
Wood, B. E., & Roux, J. A. 1982, J. Opt. Soc. Am., 72, 720
Yamada, H., & Person, W. B. 1964, J. Chem. Phys., 41, 2478